IEEE Access
Multidisciplinary | Rapid Review | Open Access Journal

Received May 25, 2020, accepted June 4, 2020, date of publication June 17, 2020, date of current version June 29, 2020.

Digital Object Identifier 10.1109/ACCESS.2020.3003076

Ultra-High-Frequency Love Surface Acoustic Wave Device for Real-Time Sensing Applications

GINA GRECO, MATTEO AGOSTINI, AND MARCO CECCHINI
NEST, Istituto Nanoscienze-CNR and Scuola Normale Superiore, 56127 Pisa, Italy

Corresponding author: Marco Cecchini (marco.cecchini@nano.cnr.it)

This work was supported by the project GLIOMICS (Proteomics/genomics/metabolomics for the biomarkers identification and the development of an ultrasensitive sensing platform to be used with peripheral fluids for glioblastoma multiforme cancer) funded by Regione Toscana under the call PAR FAS 2007-2013.

ABSTRACT Love surface acoustic wave (L-SAW) devices are ideal for real-time sensing applications. High miniaturization and sensitivity are desirable in particular for point of care diagnostics or on-site measurements. It is possible to enhance both these parameters by increasing the working frequency of these devices, but this is still a challenge. Indeed, the ultra-high frequency (UHF) range has not been explored yet for L-SAW sensing devices because it requires non-trivial fabrication and measurement setup. Here, we present a multiplexable, highly miniaturized UHF L-SAW device for real-time sensing applications. The sensor performance was first tested with mixtures of different volume percentages of isopropyl alcohol (IPA) in water. Measurements of phase and amplitude (related to change of density and viscosity, respectively) show higher sensitivity and dynamic range than a representative 100 MHz L-SAW sensor. Then, we measured the adsorption kinetics of three different concentrations of bovine serum albumin (BSA) in water on the sensor surface, demonstrating biomolecule detection. The all-electrical readout system as long as the small dimensions make the presented device particularly promising for portable UHF sensing platforms. Nonetheless, the higher sensitivity and dynamic range obtained with respect to a representative 100 MHz L-SAW sensor as long as the real-time measurements of the BSA adsorption (with an estimated limit of detection of 90 ng/mm^2) show that UHF Love SAW sensors have the potential to be used for bio-sensing applications, such as point of care diagnostics.

INDEX TERMS Biosensors, surface acoustic waves, ultra-high frequency, microfluidics.

I. INTRODUCTION

Over the last decades, the surface acoustic wave (SAW) technology has attracted the attention of the scientific community developing lab-on-chips (LOCs) [1]–[4]. LOCs are devices not bigger than few square centimeters that integrate one or more laboratory functions in a single chip. In this context, SAW-based devices have been extensively explored for controlling and actuating particles and fluids in the microfluidic regime [5]–[10]. They are also useful tools for cell manipulation [11]–[14] and for the enhancement of microfluidic sensor functionalization [15], [16]. These systems have the advantage of being fast, cheap, portable, wirelessly addressable and easy to operate. Moreover, they have the potential to be combined with the CMOS technology for developing integrated platforms [3], [17]. SAW devices have also gained particular interest for bio-sensing applications, such as environmental analysis [18]–[20], food safety control [21], [22] and point-of-care diagnostics [23]–[25]. SAWs can be divided in two main types, depending on their polarization: Rayleigh (R) and Love (L) SAWs, vertically and horizontally polarized with respect to the crystal surface, respectively. Typical working frequencies of SAW sensors are in the range of 10–300 MHz. However, it is expected that the sensor sensitivity can increase with the working frequency [26]. For example, our group recently introduced an ultra-high-frequency (UHF) R-SAW resonator biosensor that reached a limit of detection (LoD) far better than that of standard commercial quartz crystal microbalances (QCMs) [27]. Nonetheless, R-SAWs can only operate in dry conditions, which hinders their use for real-time detection in liquids. L-SAWs, thanks to their shear-horizontal polarization, do not couple

The associate editor coordinating the review of this manuscript and approving it for publication was Navanietha Krishnaraj Rathinam.

This work is licensed under a Creative Commons Attribution 4.0 License. For more information, see https://creativecommons.org/licenses/by/4.0/

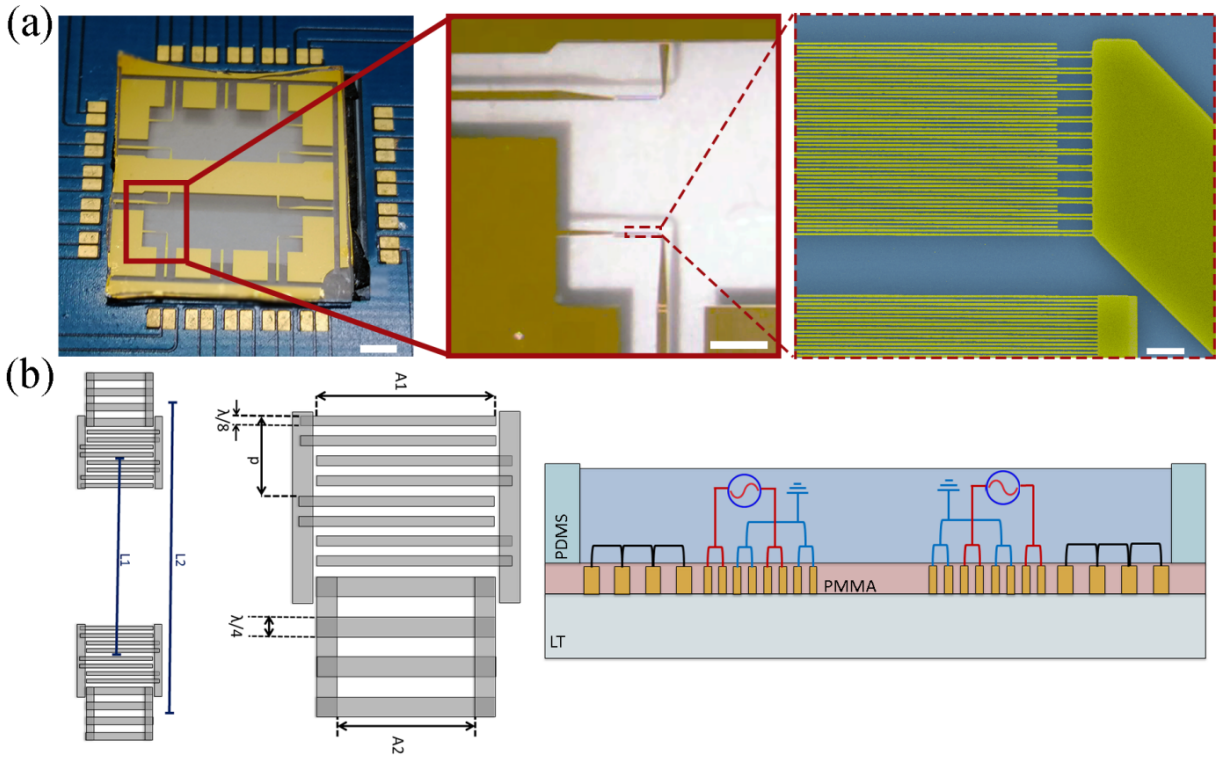

FIGURE 1. Chip illustration and electrical connections. (a) Schematics of the UHF L-SAW device. (a) Photograph of a representative device connected to a PCB for electrical readout (scale bar is 3 mm). The first inset is a zoomed image of one of the 4 sensors consisting in a delay line composed by two IDTs and two reflectors (scale bar is 1 mm). The second inset is a representative scanning electron microscopy detail of an IDT and a reflector (scale bar is 10 μm). (b) Sensor schematics. L1 and L2 represent the IDT-IDT distance and the reflectors distance, respectively. A1 and A2 represents the apertures of the IDTs and reflectors, respectively. IDTs electrodes have a width of λ /8 (split-finger configuration) and reflectors electrodes have a width of λ/4. A cross section of the sensor is shown in the bottom right panel (not to scale).

with liquids and are thus compatible with measurements in wet conditions. Another advantage of L-SAW biosensors is the presence of the waveguide layer, that has also a protective role for the interdigital transducers (IDTs) from possible external deterioration sources. If soluble polymers are chosen as waveguide layers, multiple uses of each device can be easily made by cleaning them off with their solvents [28]. More in general, it has been suggested that L-SAW devices are one of the best technologies for biosensing [29], [30]. They have been exploited for the detection of proteins and nucleic acids [31]–[36], cell growth [37]–[40] and organic molecules [41], [42]. To date, the UHF range (from 300 MHz to 3 GHz) has not been explored yet for L-SAW sensors.

Here, we demonstrate the first UHF L-SAW device for real-time sensing applications. The technology here exploited is suitable for the integration with standard CMOS devices and wirelessly addressable.

II. THE DEVICE

A. DEVICE DESIGN AND REALIZATION

The chip consists of a 2 cm $\times$ 2 cm substrate of 36° YX $LiTaO_3$ (LT) on which four delay lines (DLs) were fabricated (Figure 1a) in order to enable multiplexed measurements. Following the analytical design rules, reported for example in [43], we aimed at maximizing the Love wave generation and transmission in order to ensure a proper electro-mechanical configuration for the biosensing experiments. Each DL (the red box in Figure 1a, and schematized in details in Figure 1b) consists in two split-finger IDTs (12.5 finger pairs, metallization ratio = 50%) and two conventional $\lambda/4$ reflectors (24 fingers), where λ is the SAW wavelength. Both IDTs and reflectors were fabricated by depositing a Ti/Au (15 nm/140 nm) bilayer on the LT substrate and have 4.16 μm periodicity (p), corresponding to λ. The nominal resonance frequency f_0 is 1 GHz. Split-fingers width is 520 nm, whereas the reflectors electrodes width is 1.04 μm. IDTs and reflectors acoustic apertures are 800 μm (A1) and 900 μm (A2), respectively. The reflector distance (L1) is 2.08 mm and the delay line length (L2) is 2 mm (see the schematics in Figure 1b). Split-finger IDTs and the reflector design were chosen to avoid reflections and to improve the frequency response of the L-SAW device [29]. For the chip fabrication detailed protocol refer to the Supplementary Material. IDT impedance matching (50 Ω) was achieved by tuning the split-finger IDT aperture and the number of finger pairs [44] and verified by device testing. The DLs were connected via coplanar waveguides and wire bonded to a printed circuit board (PCB). In order to produce Love waves, a waveguide layer must be added to the

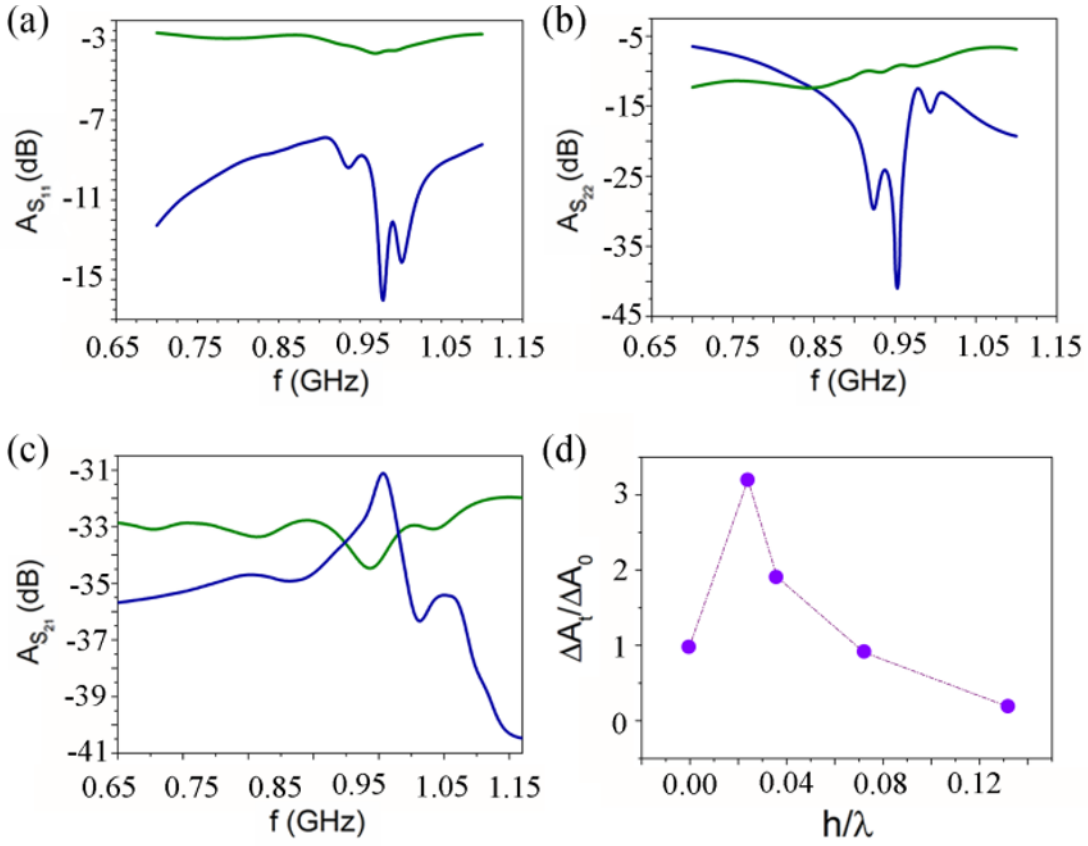

FIGURE 2. Device electrical characterization and waveguide thickness optimization. (a-b) Representative reflected power spectra of the IDTs composing the DL. (c) Representative transmitted power spectra of a DL. Green and blue lines represent, respectively, the signal with and without the optimized waveguide layer. Resonant frequency $f_0 = 0.955$ GHz. (d) Normalized transmitted power signal at f_0 at increasing PMMA waveguide thicknesses. Optimal power transmittance was achieved for a thickness of ∼125 nm.

LT chip whose 36° YX cut supports surface skimming bulk waves [45]. Polymethyl methacrylate (PMMA) was selected as the waveguide material. The use of polymers is interesting from the point of view of the sensitivity, since they have low shear velocity (1200 m/s in the case of PMMA). Another advantage of using PMMA is their easy and clean removal. In this case the waveguide layer thickness optimization can be much more straightforward than for waveguides that can't be removed without damaging the chip [29]. The PMMA waveguide layers were deposited on the device by spin-coating solutions of PMMA (950 000 g/mol) in anisole. The polymer layers were then cured at room temperature overnight. Depending on the spin speed and PMMA concentration, waveguide thicknesses in the range of 50-550 nm were obtained, as determined by profilometry measurements. A polydimethylsiloxane (PDMS) well was placed by conformal bonding on each DLs to confine the fluid on the sensing area [46]. The well was made by manually punching a 5-mm-diameter hole into the PDMS. After filling the well with the solution (25 μL), it was covered with a glass coverslip to prevent unwanted evaporation during the experiments.

B. CHARACTERIZATION AND OPTIMIZATION

For the electrical measurements, we used a vector network analyzer (VNA, ENA Series Network Analyzer, E5071C, Agilent). Each measurement was acquired by averaging 5 spectra with an intermediate frequency bandwidth of 70 kHz. First, we tested the L-SAW device by measuring the reflected power spectrum of the two IDTs of each DL. Figure 2a and Figure 2b show the reflected power spectra S11 and S22, respectively, of a representative DL before (green line in Fig. 2a and b) and after (blue line in Fig. 2a and b) waveguide thickness optimization. Figure 2c shows the transmitted power spectra before and after waveguide thickness optimization of a representative DL where the SAW resonance is identified at f = 0.955 GHz. The resonance frequency was calculated by prior smoothing the transmitted power spectrum and then extrapolating its maximum (see Supplementary material for further details). Figure 2d shows the normalized transmitted power variation of the L-SAW devices in correspondence of the resonance frequency of the DL as a function of the PMMA layer thickness. The normalized transmitted amplitude at the resonance frequency *vs.* waveguide thickness has a peak in correspondence of the

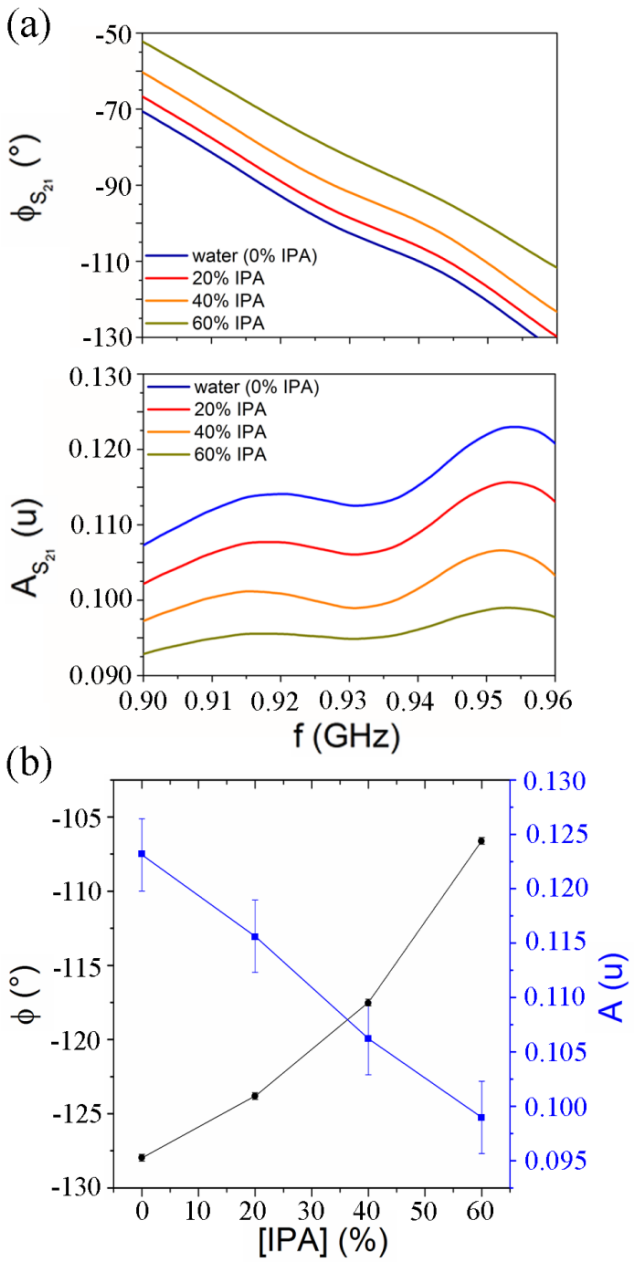

FIGURE 3. Sensor performance characterization. (a) Representative transmitted phase and power spectra at increasing concentrations of IPA in water. (c) Transmitted phase (black squares) and power (blue circles) signals at f_0 for increasing concentrations of IPA in water.

optimal SAW transmission (S21) along the DL where maximal sensitivity is consequently expected [47]–[49]. It can be seen that the curve in Figure 2d has a maximum at the waveguide thickness of ∼125 nm, indicating this value as the optimal thickness for maximizing the sensor mass sensitivity. More specifically, this waveguide ensures that more than the 99% of the injected power is transmitted through the DL.

III. SENSING EXPERIMENTS

A. DENSITY/VISCOSITY SENSING

The UHF L-SAW sensor performance was first tested with mixtures of different volume percentages of isopropyl alcohol (IPA) in water. As the volume of IPA increases, the density of the solutions decreases whereas the viscosity increases. The phase and the amplitude of L-SAW devices are highly sensitive to mass and viscosity changes [50]. We obtained phase and amplitude response curves by measuring the transmitted spectra at different IPA concentrations in water (Figure 3a). Figure 3b shows the transmitted phase (black circles) and amplitude (blue squares) at the resonant frequency of the sensor for increasing IPA concentration in water. Error bars were calculated as the standard deviation of the sensor signal over the experiment time. Comparing the phase and amplitude trends with the ones reported for a representative 100 MHz L-SAW sensor, we observe that our UHF L-SAW sensor has a higher dynamic range and a higher sensitivity to density changes. In particular, it resulted in a 2.5-fold improvement of the sensitivity with respect to [51] (see Supplementary Material for more details), suggesting that UHF devices can perform better than standard low frequency sensors.

TABLE 1. Parameters for acquisition and data processing.

Parameter	Description	Value
Δt	time interval between software acquisitions	8 s
τ	software acquisition time	12 s
N	number of points in frequency per spectrum	1601
IF-BW	intermediate frequency bandwidth	70 kHz
f_0	center frequency	0.955 GHz
f_{SPAN}	frequency span	200 MHz
s	smoothing	1.5%
P	RF power	0 dBm

B. BIO-SENSING

We tested the UHF L-SAW sensor with a biological analyte: bovine serum albumin (BSA). We tested three different concentrations of BSA in water: 0.1 mg/ml, 1 mg/mL and 10 mg/ml. BSA was chosen since serum albumin is the most plentiful protein in blood plasma; in particular, it plays a very important role in maintaining the oncotic pressure of blood and its concentration is considered a reliable sign of health (i.e., it is a critical indicator for kidney damage) [52]. We injected 25 μL of the BSA solution into the PDMS well on top of a sensor area at time t = 0 and we monitored the signal for 800 s to follow the protein adsorption kinetics up to its saturation on the sensor surface. We followed this procedure for each concentration. Considering that the well diameter is 5 mm, that we injected 25 μl of protein solution and that it is known from literature that about 70% of BSA is adsorbed onto PMMA [12], we can estimate that the surface protein density that we measured in the case of the smallest BSA concentration (0.1 mg/ml) was 90 ng/mm^2. A custom-made LabView® software was developed to

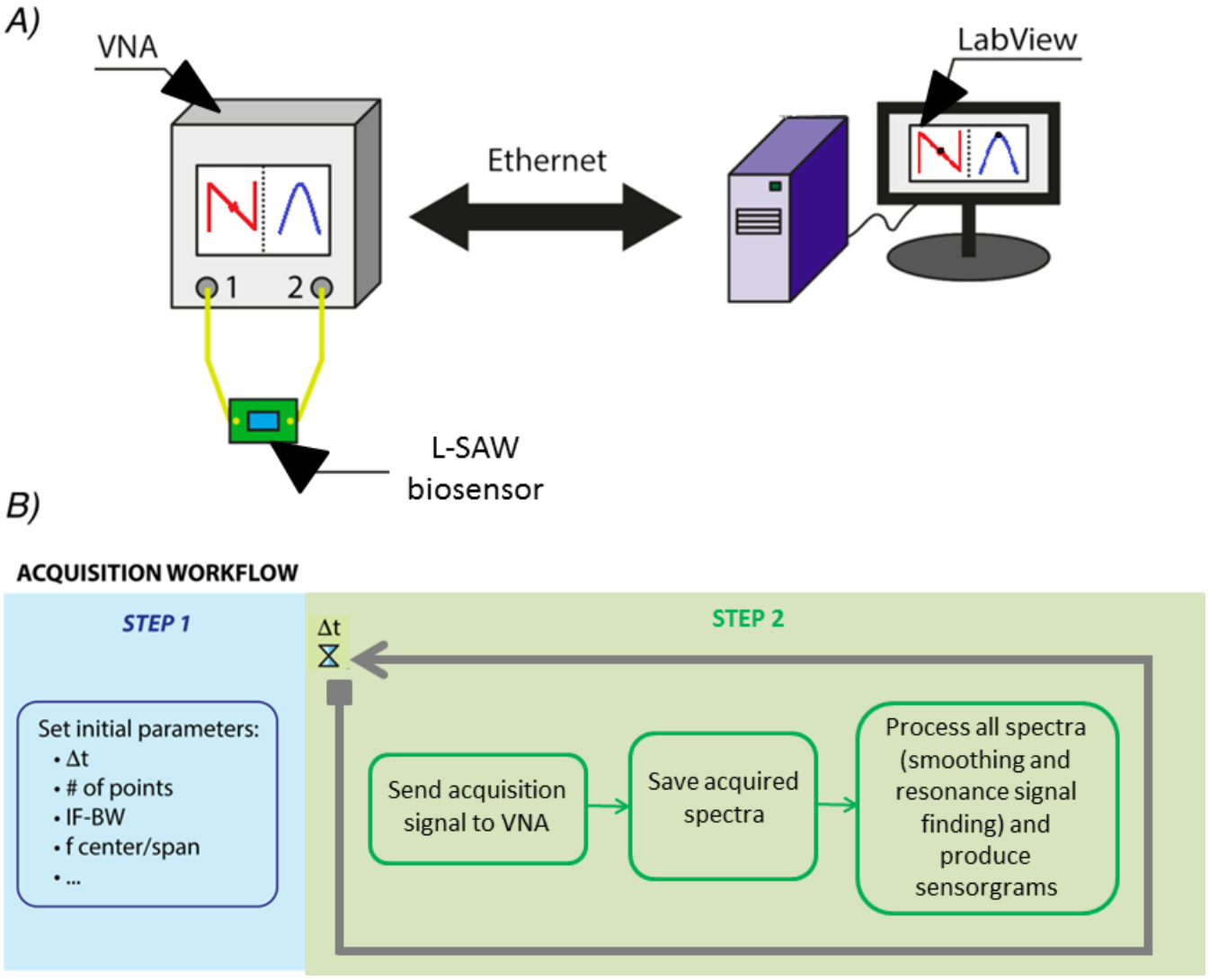

FIGURE 4. Experimental setup and algorithms. A) Scheme of the experimental setup: the device under test (DUT) is measured by a VNA acquiring two RF reflected power spectra (S11 and S22) and one transmitted spectrum (S21) per sensor. The VNA communicates with a LabView® custom-made software for spectra acquisition and data analysis (*i.e.*, smoothing and resonance signal finding). B) LabView custom software workflow. The acquisition starts with the user input of the initial parameters. Next, the software loops with Δt interval, repeating spectra collection and saving. Resonance signal finding is applied to the smoothed spectra to generate the sensorgrams.

collect and process the transmitted phase spectra from the VNA. The signal was acquired every 20 s. Table 1 reports the fundamental parameters for the acquisition and data processing that were used for the bio-sensing experiments, and figure 4 reports the experimental setup and software algorithms.

A schematic of the modification of the sensor surface and its phase response over time is depicted in Figure 5a and Figure 5b. Figure 5c shows the transmitted phase signal at the resonance frequency during BSA adsorption on the sensor surface at the three concentrations tested. Black, red and blue dots represent the phase shift over time due to 0.1 mg/ml, 1 mg/ml and 10 mg/ml BSA concentration, respectively. In order to compare our results with existing literature, data were fitted with an exponential curve. This analytical description allows us to estimate the characteristic time (τ) of the observed phenomena (Adj. R-square ≥ 0.98). As shown in the inset of Figure 5c, the characteristic times (140 s, 23 s and 10 s for 0.1 mg/ml, 1 mg/ml and 10 mg/ml, respectively) followed the expected trend $\boldsymbol{\tau} \propto \frac{1}{C_0}$, where $\boldsymbol{c_0}$ is the injected BSA concentration. The analytical description of the BSA adsorption is therefore consistent with what found in literature [53], [54]. All experiments started after a step of sensor conditioning in water that was necessary for signal stabilization. By estimating the LoD as 3σ (where σ is the standard deviation of the blank) [55] we obtained a LoD of 50 μg/ml.

The estimated LoD of 50 μg/ml along with its all-electrical readout system demonstrate that this device has all the potential to be used for bio-sensing applications, such as point of

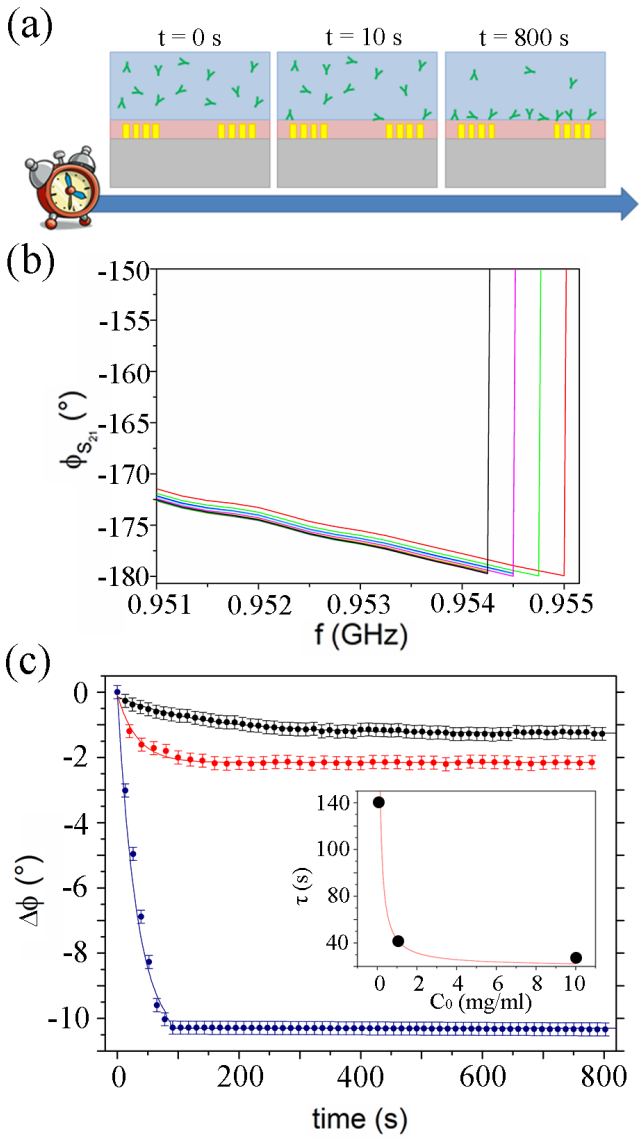

FIGURE 5. Real-time detection of BSA adsorption. (a) Schematics of the BSA adsorption timeline. Time t = 0 s refers to the injection of the solution on the sensor. t = 800 s refers to the BSA saturation condition on the sensor area. Representative transmitted phase spectra during the experiment are shown in (b). The phase shift is determined by the mass loading of the BSA on the sensor surface. (c) Black, red and blue dots represent resonance frequency phase shifts upon the adsorption of 0.1 mg/ml, 1 mg/ml and 10 mg/ml BSA solutions, respectively. Black, red and blue lines are exponential fit of the phase shift of the transmitted power at f_0 during the BSA adsorption. The inset shows the characteristic adsorption times (τ) of the three kinetics vs. the initial concentration of BSA in the solution. Red line represents the expected trend of these data.

care diagnostics and on-site measurements. In particular, this sensor is compatible with the range of variation of serum albumin as biomarker for risk prediction in various clinical conditions.

IV. CONCLUSION

In conclusion, we realized a highly miniaturized UHF L-SAW sensor. The sensor is designed to be compatible with multiplexed measurements and to be easily integrated into microfluidic systems. The all-electrical readout system and wireless addressability typical of SAW devices -as shown for example in [33], [56], along with its sensing performance make this UHF L-SAW device highly suitable for many sensing applications, For example, on-site and point of care (PoC) analyses are feasible with the presented device, opening promising perspectives for highly sensitive and portable UHF Love-SAW platforms.

REFERENCES

[1] J. Wu, Z. He, Q. Chen, and J.-M. Lin, "Biochemical analysis on microfluidic chips," *TrAC Trends Anal. Chem.*, vol. 80, pp. 213–231, Jun. 2016.
[2] D. Erickson, D. O'Dell, L. Jiang, V. Oncescu, A. Gumus, S. Lee, M. Mancuso, and S. Mehta, "Smartphone technology can be transformative to the deployment of lab-on-chip diagnostics," *Lab Chip*, vol. 14, no. 17, pp. 3159–3164, 2014.
[3] X. Ding, P. Li, S.-C. S. Lin, Z. S. Stratton, N. Nama, F. Guo, D. Slotcavage, X. Mao, J. Shi, F. Costanzoa, and T. J. Huang, "Surface acoustic wave microfluidics," *Lab Chip*, vol. 13, no. 18, pp. 3626–3649, 2013.
[4] D. B. Go, M. Z. Atashbar, Z. Ramshani, and H.-C. Chang, "Surface acoustic wave devices for chemical sensing and microfluidics: A review and perspective," *Anal. Methods*, vol. 9, no. 28, pp. 4112–4134, 2017.
[5] K. Kustanovich, V. Yantchev, A. Olivefors, B. Ali Doosti, T. Lobovkina, and A. Jesorka, "A high-performance lab-on-a-chip liquid sensor employing surface acoustic wave resonance: Part II," *J. Micromech. Microeng.*, vol. 29, no. 2, Feb. 2019, Art. no. 024001.
[6] R. J. Shilton, M. Travagliati, F. Beltram, and M. Cecchini, "Nanoliter-droplet acoustic streaming via ultra high frequency surface acoustic waves," *Adv. Mater.*, vol. 26, pp. 4941–4946, Aug. 2014.
[7] R. J. Shilton, M. Travagliati, F. Beltram, and M. Cecchini, "Microfluidic pumping through miniaturized channels driven by ultra-high frequency surface acoustic waves," *Appl. Phys. Lett.*, vol. 105, no. 7, Aug. 2014, Art. no. 074106.
[8] S. Meucci, I. Tonazzini, F. Beltram, and M. Cecchini, "Biocompatible noisy nanotopographies with specific directionality for controlled anisotropic cell cultures," *Soft Matter*, vol. 8, no. 4, pp. 1109–1119, 2012.
[9] R. J. Shilton, V. Mattoli, M. Travagliati, M. Agostini, A. Desii, F. Beltram, and M. Cecchini, "Rapid and controllable digital microfluidic heating by surface acoustic waves," *Adv. Funct. Mater.*, vol. 25, no. 37, pp. 5895–5901, Oct. 2015.
[10] L. Masini, M. Cecchini, S. Girardo, R. Cingolani, D. Pisignano, and F. Beltram, "Surface-acoustic-wave counterflow micropumps for on-chip liquid motion control in two-dimensional microchannel arrays," *Lab Chip*, vol. 10, no. 15, pp. 1997–2000, 2010.
[11] G. Greco, M. Agostini, I. Tonazzini, D. Sallemi, S. Barone, and M. Cecchini, "Surface-acoustic-wave (SAW)-driven device for dynamic cell cultures," *Anal. Chem.*, vol. 90, pp. 7450–7457, May 2018.
[12] M. Wiklund, "Acoustofluidics 12: Biocompatibility and cell viability in microfluidic acoustic resonators," *Lab Chip*, vol. 12, no. 11, pp. 2018–2028, May 2012.
[13] A. Ozcelik, N. Nama, P.-H. Huang, M. Kaynak, M. R. McReynolds, W. Hanna-Rose, and T. J. Huang, "Acoustofluidics: Acoustofluidic rotational manipulation of cells and organisms using oscillating solid structures," *Small*, vol. 12, no. 37, p. 5230, 2016.
[14] F. Guo, P. Li, J. B. French, Z. Mao, H. Zhao, S. Li, N. Nama, J. R. Fick, S. J. Benkovic, and T. J. Huang, "Controlling cell-cell interactions using surface acoustic waves," *Proc. Nat. Acad. Sci. USA*, vol. 112, no. 1, pp. 43–48, Jan. 2015.
[15] G. Greco, M. Agostini, R. Shilton, M. Travagliati, G. Signore, and M. Cecchini, "Surface acoustic wave (SAW)-enhanced chemical functionalization of gold films," *Sensors*, vol. 17, no. 11, pp. 1–11, 2017.
[16] A. Sonato, M. Agostini, G. Ruffato, E. Gazzola, D. Liuni, G. Greco, M. Travagliati, M. Cecchini, and F. Romanato, "A surface acoustic wave (SAW)-enhanced grating-coupling phase-interrogation surface plasmon resonance (SPR) microfluidic biosensor," *Lab Chip*, vol. 16, no. 7, pp. 1224–1233, 2016.
[17] G. Destgeer and H. J. Sung, "Recent advances in microfluidic actuation and micro-object manipulation via surface acoustic waves," *Lab Chip*, vol. 15, no. 13, pp. 2722–2738, 2015.

[18] K. M. M. Kabir, B. Lay, A. E. Kandjani, Y. M. Sabri, S. J. Ippolito, and S. K. Bhargava, "A nanoengineered surface acoustic wave device for analysis of mercury in gas phase," *Sens. Actuators B, Chem.*, vol. 234, pp. 562–572, Oct. 2016.

[19] A. Gupta, P. Kumar, and S. Pandey, "Analysis of multilayered SAW based gas sensor," in *Proc. Int. Conf. Trends Electron. Informat. (ICEI)*, May 2017, pp. 239–242.

[20] Z. Tang, W. Wu, J. Gao, and P. Yang, "Feasibility study on wireless passive SAW sensor in IoT enabled water distribution system," in *Proc. IEEE Int. Conf. Internet Things (iThings) IEEE Green Comput. Commun. (GreenCom) IEEE Cyber, Phys. Social Comput. (CPSCom) IEEE Smart Data (SmartData)*, Jun. 2017, pp. 830–834.

[21] Z. Bilkova and J. Ku, "Love wave fully integrated lab-on-chip platform for food pathogen detection—LOVE-FOOD," Eur. Project, Tech. Rep. 317742, 2014, pp. 1–13. [Online]. Available: https://cordis.europa.eu/docs/projects/cnect/2/317742/080/deliverables/001-LoveFoodD35.pdf

[22] A. López-Gómez, F. Cerdán-Cartagena, J. Suardíaz-Muro, M. Boluda-Aguilar, M. E. Hernández-Hernández, M. A. López-Serrano, and J. López-Coronado, "Radiofrequency identification and surface acoustic wave technologies for developing the food intelligent packaging concept," *Food Eng. Rev.*, vol. 7, no. 1, pp. 11–32, Mar. 2015.

[23] J. Lee, Y.-S. Choi, Y. Lee, H. J. Lee, J. N. Lee, S. K. Kim, K. Y. Han, E. C. Cho, J. C. Park, and S. S. Lee, "Sensitive and simultaneous detection of cardiac markers in human serum using surface acoustic wave immunosensor," *Anal. Chem.*, vol. 83, no. 22, pp. 8629–8635, Nov. 2011.

[24] W. Lee, J. Jung, Y. K. Hahn, S. K. Kim, Y. Lee, J. Lee, T.-H. Lee, J.-Y. Park, H. Seo, J. N. Lee, J. H. Oh, Y.-S. Choi, and S. S. Lee, "A centrifugally actuated point-of-care testing system for the surface acoustic wave immunosensing of cardiac troponin I," *Analyst*, vol. 138, no. 9, pp. 2558–2566, 2013.

[25] G. Papadakis, J. M. Friedt, M. Eck, D. Rabus, G. Jobst, and E. Gizeli, "Optimized acoustic biochip integrated with microfluidics for biomarkers detection in molecular diagnostics," *Biomed. Microdevices*, vol. 19, no. 3, pp. 1–11, Sep. 2017.

[26] F. L. Dickert, P. Forth, W.-E. Bulst, G. Fischerauer, and U. Knauer, "SAW devices-sensitivity enhancement in going from 80 MHz to 1 GHz," *Sens. Actuators B, Chem.*, vol. 46, no. 2, pp. 120–125, Feb. 1998.

[27] M. Agostini, G. Greco, and M. Cecchini, "A Rayleigh surface acoustic wave (R-SAW) resonator biosensor based on positive and negative reflectors with sub-nanomolar limit of detection," *Sens. Actuators B, Chem.*, vol. 254, pp. 1–7, Jan. 2018.

[28] Z. Xu and Y. J. Yuan, "Implementation of guiding layers of surface acoustic wave devices: A review," *Biosensors Bioelectron.*, vol. 99, pp. 500–512, Jan. 2018.

[29] M. I. G. Rocha, Y. Jimenez, F. A. Laurent, and A. Arnau, "Love wave biosensors: A review," in *State of the Art in Biosensors-General Aspects*. Rijeka, Croatia: InTech, 2013.

[30] I. Voiculescu and A. N. Nordin, "Acoustic wave based MEMS devices for biosensing applications," *Biosensors Bioelectron.*, vol. 33, no. 1, pp. 1–9, Mar. 2012.

[31] S. Lee, K.-B. Kim, and Y.-I. Kim, "Love wave SAW biosensors for detection of antigen-antibody binding and comparison with SPR biosensor," *Food Sci. Biotechnol.*, vol. 20, no. 5, pp. 1413–1418, Nov. 2011.

[32] M. Gianneli, K. Tsougeni, A. Grammoustianou, A. Tserepi, E. Gogolides, and E. Gizeli, "Nanostructured PMMA-coated love wave device as a platform for protein adsorption studies," *Sens. Actuators B, Chem.*, vol. 236, pp. 583–590, Nov. 2016.

[33] H. Oh, C. Fu, K. Kim, and K. Lee, "Wireless and simultaneous detections of multiple bio-molecules in a single sensor using love wave biosensor," *Sensors*, vol. 14, no. 11, pp. 21660–21675, Nov. 2014.

[34] G. Kovacs, M. J. Vellekoop, R. Haueis, G. W. Lubking, and A. Venema, "A love wave sensor for (bio)chemical sensing in liquids," *Sens. Actuators A, Phys.*, vol. 43, nos. 1–3, pp. 38–43, May 1994.

[35] V. Blondeau-Patissier, W. Boireau, B. Cavallier, G. Lengaigne, W. Daniau, G. Martin, and S. Ballandras, "Integrated love wave device dedicated to biomolecular interactions measurements in aqueous media," *Sensors*, vol. 7, no. 9, pp. 1992–2003, Sep. 2007.

[36] F. Di Pietrantonio, M. Benetti, D. Cannatà, E. Verona, M. Girasole, M. Fosca, S. Dinarelli, M. Staiano, V. M. Marzullo, A. Capo, A. Varriale, and S. D'Auria, "A shear horizontal surface acoustic wave biosensor for a rapid and specific detection of d-serine," *Sens. Actuators B, Chem.*, vol. 226, pp. 1–6, Apr. 2016.

[37] X. Zhang, J. Fang, L. Zou, Y. Zou, L. Lang, F. Gao, N. Hu, and P. Wang, "A novel sensitive cell-based love wave biosensor for marine toxin detection," *Biosensors Bioelectron.*, vol. 77, pp. 573–579, Mar. 2016.

[38] Y. W. Kim, S. E. Sardari, M. T. Meyer, A. A. Iliadis, H. C. Wu, W. E. Bentley, and R. Ghodssi, "An ALD aluminum oxide passivated surface acoustic wave sensor for early biofilm detection," *Sens. Actuators B, Chem.*, vol. 163, no. 1, pp. 136–145, Mar. 2012.

[39] Y. Wook Kim, S. E. Sardari, A. A. Iliadis, and R. Ghodssi, "A bacterial biofilm surface acoustic wave sensor for real time biofilm growth monitoring," in *Proc. IEEE Sensors*, Nov. 2010, pp. 1568–1571.

[40] D. W. Branch and S. M. Brozik, "Low-level detection of a bacillus anthracis simulant using love-wave biosensors on 36°YX $LiTaO_3$," *Biosensors Bioelectron.*, vol. 19, no. 8, pp. 849–859, Mar. 2004.

[41] L. Rana, R. Gupta, M. Tomar, and V. Gupta, "Highly sensitive love wave acoustic biosensor for uric acid," *Sens. Actuators B, Chem.*, vol. 261, pp. 169–177, May 2018.

[42] D. Matatagui, M. J. Fernández, J. Fontecha, J. P. Santos, I. Gràcia, C. Cané, and M. C. Horrillo, "Love-wave sensor array to detect, discriminate and classify chemical warfare agent simulants," *Sens. Actuators B, Chem.*, vol. 175, pp. 173–178, Dec. 2012.

[43] D. Ballantine, R. White, S. Martin, A. Ricco, E. Zellers, G. Frye, and H. Wohltjen, *Acoustic Wave Sensors*. San Diego, CA USA: Academic, 1997.

[44] M. K. Ekström, T. Aref, J. Runeson, J. Björck, I. Boström, and P. Delsing, "Surface acoustic wave unidirectional transducers for quantum applications," *Appl. Phys. Lett.*, vol. 110, no. 7, pp. 1–5, 2017.

[45] K. A. Melzak and E. Gizeli, "Love wave biosensors," in *Handbook of Biosensors and Biochips*. Hoboken, NJ, USA: Wiley, 2008.

[46] C. Caliendo and M. Hamidullah, "Guided acoustic wave sensors for liquid environments," *J. Phys. D, Appl. Phys.*, vol. 52, no. 15, Apr. 2019, Art. no. 153001.

[47] E. Gizeli, "Study of the sensitivity of the acoustic waveguide sensor," *Anal. Chem.*, vol. 72, no. 24, pp. 5967–5972, Dec. 2000.

[48] F. Josse, F. Bender, and R. W. Cernosek, "Guided shear horizontal surface acoustic wave sensors for chemical and biochemical detection in liquids," *Anal. Chem.*, vol. 73, no. 24, pp. 5937–5944, Dec. 2001.

[49] W. Wang and S. He, "Sensitivity evaluation of a love wave sensor with multi-guiding-layer structure for biochemical application," *Sensors Transducers*, vol. 96, no. 9, pp. 32–41, 2008.

[50] K. A. Melzak and E. Gizeli, "Love wave biosensors," in *Handbook of Biosensors and Biochips*. Hoboken, NJ, USA: Wiley, 2008.

[51] B. Jakoby and M. J. Vellekoop, "Viscosity sensing using a love-wave device," *Sens. Actuators A, Phys.*, vol. 68, nos. 1–3, pp. 275–281, Jun. 1998.

[52] M. Chen, X. Xiang, K. Wu, H. He, H. Chen, and C. Ma, "A novel detection method of human serum albumin based on the poly(thymine)-templated copper nanoparticles," *Sensors*, vol. 17, no. 11, p. 2684, Nov. 2017.

[53] C. Liu and B. J. Meenan, "Effect of air plasma processing on the adsorption behaviour of bovine serum albumin on spin-coated PMMA surfaces," *J. Bionic Eng.*, vol. 5, no. 3, pp. 204–214, Sep. 2008.

[54] N. F. Y. Durand and P. Renaud, "Label-free determination of protein-surface interaction kinetics by ionic conductance inside a nanochannel," *Lab Chip*, vol. 9, no. 2, pp. 319–324, 2009.

[55] A. Shrivastava and V. Gupta, "Methods for the determination of limit of detection and limit of quantitation of the analytical methods," *Chronicles Young Scientists*, vol. 2, no. 1, p. 21, 2011.

[56] F. Lurz, T. Ostertag, B. Scheiner, R. Weigel, and A. Koelpin, "Reader architectures for wireless surface acoustic wave sensors," *Sensors*, vol. 18, no. 6, p. 1734, May 2018.

GINA GRECO was born in Italy, in 1990. She received the M.S. degree in physics (medical physics curriculum) from the University of Pisa, Italy, in 2015. She is currently pursuing the Ph.D. degree in biophysical sciences with the National Enterprise for Nanoscience and Nanotechnology (NEST) Laboratory, Scuola Normale Superiore, Pisa.

Her current research interests are surface acoustic wave (SAW) biosensors, SAW-driven microfluidic systems, and the development of new devices for early detection of diseases and cell cultures.

MATTEO AGOSTINI was born in Latina, Italy, in 1988. He received the B.S. degree in electronics engineering and the M.S. degree in nanotechnology engineering from the La Sapienza–University of Rome and the Ph.D. degree in molecular biophysics with a thesis on SAW-biosensors and microfluidic devices for life science applications from Scuola Normale Superiore, Pisa, Italy, in 2018. Since 2017, he has been a Research Fellow of Scuola Normale Superiore. His activities are based in the National Enterprise for Nanoscience and Nanotechnology (NEST) Laboratory, Pisa, where he studies and develops SAW-based nano-devices for sensing and microfluidics applications. He is an expert of micro- and nano-fabrication techniques, sensors development and characterization, and biosensing systems. He also explores the chemical functionalization of surfaces for several applications, sensing, and hydrophobization, among all.

MARCO CECCHINI was born in Italy, in 1975. He received the master's degree in physics from the Department of Physics, University of Pisa, Pisa, Italy, in 1999, the Ph.D. degree in condensed matter physics from Scuola Normale Superiore, Pisa, Italy, in 2006, and the Laurea degree in biotechnology from the Department of Biology, University of Pisa. He is currently a Senior Researcher with the Nanoscience Institute, Italian National Research Council (CNR), Scuola Normale Superiore, and a Lecturer of biomaterial science with the University of Pisa. His main research interests are in the development of nanostructured biomaterials for brain pathologies and nerve regeneration, and the designing, production, and testing of surface-acoustic-wave driven microfluidic devices for advanced cell cultures and biosensing.